Single Spin Asymmetries in Charged Kaon Production from Semi-Inclusive Deep Inelastic Scattering on a Transversely Polarized ^{3}He Target

Y.X. Zhao,[1, *] Y. Wang,[2] K. Allada,[3, 4] K. Aniol,[5] J.R.M. Annand,[6] T. Averett,[7] F. Benmokhtar,[8] W. Bertozzi,[3] P.C. Bradshaw,[7] P. Bosted,[4] A. Camsonne,[4] M. Canan,[9] G.D. Cates,[10] C. Chen,[11] J.-P. Chen,[4] W. Chen,[12] K. Chirapatpimol,[10] E. Chudakov,[4] E. Cisbani,[13, 14] J.C. Cornejo,[5] F. Cusanno,[15] M.M. Dalton,[10] W. Deconinck,[3] C.W. de Jager,[4] R. De Leo,[16] X. Deng,[10] A. Deur,[4] H. Ding,[10] P. A. M. Dolph,[10] C. Dutta,[17] D. Dutta,[18] L. El Fassi,[19] S. Frullani,[15, 14] H. Gao,[12] F. Garibaldi,[15, 14] D. Gaskell,[4] S. Gilad,[3] R. Gilman,[4, 19] O. Glamazdin,[20] S. Golge,[9] L. Guo,[21] D. Hamilton,[6] O. Hansen,[4] D.W. Higinbotham,[4] T. Holmstrom,[22] J. Huang,[3, 21, 23] M. Huang,[12] H. F Ibrahim,[24] M. Iodice,[25] X. Jiang,[19, 21] G. Jin,[10] M.K. Jones,[4] J. Katich,[7] A. Kelleher,[7] W. Kim,[26] A. Kolarkar,[17] W. Korsch,[17] J.J. LeRose,[4] X. Li,[27] Y. Li,[27] R. Lindgren,[10] N. Liyanage,[10] E. Long,[28, 29] H.-J. Lu,[1] D.J. Margaziotis,[5] P. Markowitz,[30] S. Marrone,[16] D. McNulty,[31] Z.-E. Meziani,[32] R. Michaels,[4] B. Moffit,[3, 4] C. Muñoz Camacho,[33] S. Nanda,[4] A. Narayan,[18] V. Nelyubin,[10] B. Norum,[10] Y. Oh,[34] M. Osipenko,[35] D. Parno,[8] J.-C. Peng,[2] S. K. Phillips,[29] M. Posik,[32] A. J. R. Puckett,[3, 21] X. Qian,[12, 36, 23] Y. Qiang,[12, 4] A. Rakhman,[37] R. Ransome,[19] S. Riordan,[10] A. Saha,[4, †] B. Sawatzky,[32, 4] E. Schulte,[19] A. Shahinyan,[38] M. H. Shabestari,[10] S. Širca,[39] S. Stepanyan,[40] R. Subedi,[10] V. Sulkosky,[3, 4] L.-G. Tang,[11] A. Tobias,[10] G. M. Urciuoli,[13] I. Vilardi,[16] K. Wang,[10] B. Wojtsekhowski,[4] X. Yan,[1] H. Yao,[32] Y. Ye,[1] Z. Ye,[11] L. Yuan,[11] X. Zhan,[3] Y. Zhang,[41] Y.-W. Zhang,[41] B. Zhao,[7] X. Zheng,[10] L. Zhu,[2, 11] X. Zhu,[12] and X. Zong[12]

(The Jefferson Lab Hall A Collaboration)

[1] *University of Science and Technology of China, Hefei 230026, People's Republic of China*
[2] *University of Illinois, Urbana-Champaign, IL 61801*
[3] *Massachusetts Institute of Technology, Cambridge, MA 02139*
[4] *Thomas Jefferson National Accelerator Facility, Newport News, VA 23606*
[5] *California State University, Los Angeles, Los Angeles, CA 90032*
[6] *University of Glasgow, Glasgow G12 8QQ, Scotland, United Kingdom*
[7] *College of William and Mary, Williamsburg, VA 23187*
[8] *Carnegie Mellon University, Pittsburgh, PA 15213*
[9] *Old Dominion University, Norfolk, VA 23529*
[10] *University of Virginia, Charlottesville, VA 22904*
[11] *Hampton University, Hampton, VA 23187*
[12] *Duke University, Durham, NC 27708*
[13] *INFN, Sezione di Roma, I-00185 Rome, Italy*
[14] *Istituto Superiore di Sanità, I-00161 Rome, Italy*
[15] *INFN, Sezione di Roma, I-00161 Rome, Italy*
[16] *INFN, Sezione di Bari and University of Bari, I-70126 Bari, Italy*
[17] *University of Kentucky, Lexington, KY 40506*
[18] *Mississippi State University, Mississippi State, MS 39762*
[19] *Rutgers, The State University of New Jersey, Piscataway, NJ 08855*
[20] *Kharkov Institute of Physics and Technology, Kharkov 61108, Ukraine*
[21] *Los Alamos National Laboratory, Los Alamos, NM 87545*
[22] *Longwood University, Farmville, VA 23909*
[23] *Physics Department, Brookhaven National Laboratory, Upton, NY*
[24] *Cairo University, Giza 12613, Egypt*
[25] *INFN, Sezione di Roma Tre, I-00146 Rome, Italy*
[26] *Kyungpook National University, Taegu 702-701, Republic of Korea*
[27] *China Institute of Atomic Energy, Beijing, People's Republic of China*
[28] *Kent State University, Kent, OH 44242*
[29] *University of New Hampshire, Durham, NH 03824*
[30] *Florida International University, Miami, FL 33199*
[31] *University of Massachusetts, Amherst, MA 01003*
[32] *Temple University, Philadelphia, PA 19122*
[33] *Université Blaise Pascal/IN2P3, F-63177 Aubière, France*
[34] *Seoul National University, Seoul, South Korea*
[35] *INFN, Sezione di Genova, I-16146 Genova, Italy*
[36] *Kellogg Radiation Laboratory, California Institute of Technology, Pasadena, CA 91125*
[37] *Syracuse University, Syracuse, NY 13244*
[38] *Yerevan Physics Institute, Yerevan 375036, Armenia*
[39] *University of Ljubljana, SI-1000 Ljubljana, Slovenia*
[40] *Kyungpook National University, Taegu City, South Korea*
[41] *Lanzhou University, Lanzhou 730000, Gansu, People's Republic of China*

We report the first measurement of target single spin asymmetries of charged kaons produced in semi-inclusive deep inelastic scattering of electrons off a transversely polarized ^{3}He target. Both the Collins and Sivers moments, which are related to the nucleon transversity and Sivers distributions, respectively, are extracted over the kinematic range of $0.1<x_{bj}<0.4$ for K^+ and K^- production. While the Collins and Sivers moments for K^+ are consistent with zero within the experimental uncertainties, both moments for K^- favor negative values. The Sivers moments are compared to the theoretical prediction from a phenomenological fit to the world data. While the K^+ Sivers moments are consistent with the prediction, the K^- results differ from the prediction at the 2-sigma level.

PACS numbers: 24.70.+s, 14.20.Dh, 24.85.+p, 25.30.Rw

Significant progress has been made in recent years on our understanding of the transversity distribution as well as transverse-momentum-dependent parton distributions (TMDs) of the nucleons [1, 2]. The nucleon transversity distribution [3], which represents the correlation between the quark transverse spin and the nucleon transverse spin, is suppressed in inclusive deep inelastic scattering experiments due to its chiral-odd nature. While it was recognized that polarized Drell-Yan experiments [3, 4] and Semi-Inclusive Deep Inelastic Scattering (SIDIS) experiments can both access the transversity distribution, our current knowledge on this distribution is mainly obtained from SIDIS.

The SIDIS processes, in which a hadron is detected in coincidence with the scattered lepton [5–9], also involve another chiral-odd object, the so-called Collins fragmentation function [10], to ensure helicity conservation. This allows the extraction of the transversity distribution, provided that the Collins fragmentation function is sizable. The Collins fragmentation functions were extracted to be significant by experiments at Belle [11] and at BaBar [12].

Pioneering efforts have been devoted towards the measurement of transversity distributions by the HERMES and COMPASS collaborations in dedicated SIDIS experiments using transversely polarized targets [13–15]. A modulation of the form $\sin(\phi_h + \phi_S)$, the Collins moment, where ϕ_h and ϕ_S are the azimuthal angles of the detected hadron and the nucleon spin with respect to the lepton scattering plane, corresponds to a convolution of the transversity distribution and the Collins fragmentation function. Another important leading-twist TMD is the so-called Sivers function [16], which represents the correlation between the nucleon transverse spin and the quark transverse momentum. It can be extracted through another angular modulation called the Sivers moment with the form of $\sin(\phi_h - \phi_S)$. Although the Sivers function is odd under the time reversal operation without exchanging the initial and final states [10], it is allowed in the presence of QCD final-state interactions (FSI) between the outgoing quark and the target remnant [17–20].

* Corresponding author: yxzhao@jlab.org
† Deceased

Results from the HERMES and COMPASS experiments have clearly shown the presence of the $\sin(\phi_h + \phi_S)$ and $\sin(\phi_h - \phi_S)$ modulations from proton targets [13–15]. In remarkable contrast, much smaller modulations were found from deuteron targets [21], suggesting that the process is flavor dependent. To shed new light on the flavor structure of the transversity and Sivers functions, it is important to extend SIDIS measurements to a polarized ^{3}He target, whose spin comes predominantly from the neutron.

The first such measurement was carried out on a polarized ^{3}He target in Hall A at the Jefferson Laboratory and results for the charged pion SIDIS production have already been reported [22, 23]. In this paper, we present the results on the azimuthal asymmetries in charged kaon SIDIS production. Since kaons contain strange quarks, the role of sea quarks in the nucleons with respect to the Collins and Sivers effects can be explored. The HERMES collaboration [14] observed that the Collins effect from the proton target for K^+ is larger than that for π^+, while for K^- the Collins effect is small and consistent with zero. They also reported that the Sivers effect for K^+ from the proton target is large and positive, but very small for K^- [13]. The COMPASS collaboration reported that the Collins and Sivers effects for K^+ and K^- production from the polarized deuteron target are consistent with zero [21]. Results from this work using a polarized ^{3}He target will provide important new information to study the flavor dependent behavior of the Collins and Sivers effects.

The data were collected during experiment E06-010 at Jefferson Lab, Hall A. The experiment was conducted from November 2008 to February 2009 using a 5.9-GeV electron beam with an average current of 12 μA and a transversely polarized ^{3}He target. Scattered electrons were detected in the BigBite spectrometer which was at 30° to the beam right (facing the beam dump) with a momentum acceptance from 0.6 GeV/c to 2.5 GeV/c. Coincident charged hadrons ($\pi^\pm$, $K^\pm$ and protons) were detected in the High Resolution Spectrometer (HRS) [24], which was at 16° to the beam left with a central momentum of 2.35 GeV/c. The electron beam helicity was flipped at a rate of 30 Hz. The unpolarized beam was achieved by summing the two helicity states, which differ by less than 100ppm per 1-hour run in beam charge.

The polarized ^{3}He target consisted of a 40-cm long glass cell containing ∼10 atm of ^{3}He and a small amount

of N_2 to reduce depolarization [24, 25]. The ground state of ^{3}He nuclear wavefunction is dominated by the S-state, in which the proton spins cancel each other and the nuclear spin is mostly carried by the neutron [26]. Three pairs of Helmholtz coils were used in the experiment for producing the holding magnetic field in any direction. During the experiment, the target spin direction was oriented to transverse and vertical directions in order to enlarge the azimuthal angular coverage ϕ_S. ^{3}He nuclei were polarized by spin exchange optical pumping of a Rb-K mixture [27]. Nuclear Magnetic Resonance (NMR) measurements, calibrated by the known water NMR signal and the electron paramagnetic resonance method, were performed to monitor the target polarization while the target spin direction was flipped every 20 minutes through adiabatic fast passage. An average in-beam target polarization of $(55.4 \pm 2.8)\%$ was achieved during the experiment.

The BigBite spectrometer consisted of a single open dipole magnet, eighteen planes of multi-wire drift chambers organized in three groups and a scintillator plane sandwiched between lead-glass preshower and shower calorimeters. The magnetic field from the dipole, combined with tracking information from the drift chambers, was used to reconstruct the momenta of charged particles. Timing information for the scattered electrons was provided by the scintillators, and the electron trigger was formed by summing signals from two overlapping rows of preshower and shower blocks [28]. The angular acceptance of the BigBite spectrometer was about 64 msr for a 40-cm target, which was essential to enlarge the azimuthal angular coverage ϕ_h for hadrons, given the small ($\sim$6 msr) angular acceptance of the HRS. A clean sample of electrons was achieved by using two-dimensional cuts on the preshower energy E_{ps} and the momentum-dependent ratio E/p in which E and p are the total energy deposit in the calorimeter and the reconstructed momentum, respectively. After combining all the cuts, the π^- contamination in the electron sample was less than 1%.

The HRS spectrometer configured for hadron detection consisted of two drift chambers for tracking, two scintillator planes for timing and triggering, a CO_2 gas Cerenkov detector and two layers of lead-glass calorimeter for electron rejection, an aerogel Cerenkov detector for pion rejection, and a ring imaging Cerenkov detector for hadron (pion, kaon, proton) identification [29]. In addition, Coincidence Time Of Flight (CTOF) between scattered electrons and hadrons was also recorded for hadron identification. Fig. 1 shows the CTOF spectrum. It describes the difference between the measured time of flight of the hadron and that of the expected kaon based on the electron timing. Therefore, the kaon peak is centered at zero and the proton, which is slower than the kaon, is peaked at a negative value. By applying a "pion rejection" cut on the aerogel detector, pions were strongly suppressed, and the contamination of π^+ (π^-) in the K^+ (K^-) sample was less than 2% (5%). The ran-
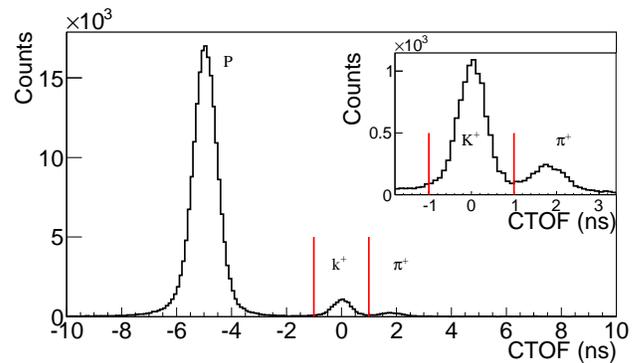

FIG. 1. (Color online) ^{3}He$(e, e'h^+)$X coincidence timing spectrum after a cut on the aerogel detector to remove pions, where h represents detected hadron. The kaon selection cuts are shown as the two vertical lines. The top right sub-plot shows only K^+ and π^+ peaks in a relatively small CTOF range.
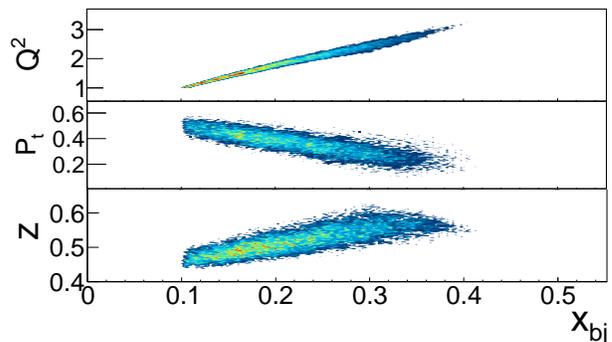

FIG. 2. (Color online) Correlation between x_{bj} and kinematics variables (Q^2, P_t, z) for K^+, where $x_{bj} = \frac{Q^2}{2P \cdot q}$, $P_t = \sqrt{\vec{P_h}^2 - (\frac{\vec{q} \cdot \vec{P_h}}{|\vec{q}|})^2}$, $z = \frac{P \cdot P_h}{P \cdot q}$, P is the four-momentum of the initial nucleon, q is the four-momentum of the virtual photon, P_h is the four-momentum of the detected hadron.

dom coincidence contamination in the K^+ (K^-) sample was less than 4% (1%), and the coincidental proton contamination in the K^+ sample was negligible.

The SIDIS event sample for the analysis was selected by requiring: 1) four-momentum-transfer squared $Q^2 > 1$ GeV^2, 2) virtual photon-nucleon invariant mass $W > 2.3$ GeV, 3) the missing mass of undetected final-state particles $W' > 1.6$ GeV. The kinematics coverage for K^+ is shown in Fig. 2. After all the cuts, the total number of accepted SIDIS events were about 10k and 2k for K^+ and K^-, respectively. The data were analyzed by using an azimuthally unbinned Maximum Likelihood Estimator (MLE) [30]. Due to the low statistics of the K^- sample, the data were binned in one kinematical bin, while for K^+, the data were binned in four bins of x_{bj}. The central values for various kinematical variables are listed in Table I.

	x_{bj}	y	z	Q^2 GeV^2	P_t GeV	W GeV	W' GeV
K^+	0.137	0.85	0.48	1.29	0.46	3.0	2.08
K^+	0.190	0.81	0.51	1.69	0.40	2.85	1.96
K^+	0.250	0.77	0.53	2.11	0.33	2.69	1.83
K^+	0.324	0.73	0.56	2.60	0.26	2.51	1.69
K^-	0.210	0.80	0.51	1.83	0.38	2.80	1.93

TABLE I. Tabulated central values for kinematical variables x_{bj}, y, Q^2, z, P_t, W, W', where $y = \frac{q \cdot P}{l \cdot P}$, $W = \sqrt{(P+q)^2}$, $W' = \sqrt{(q+P-P_h)^2}$, and l is the four-momentum of the incoming lepton.
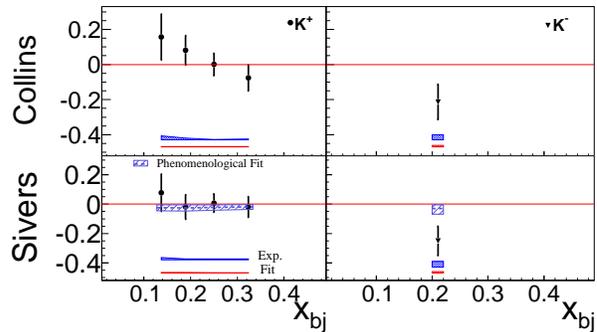

FIG. 3. (Color online) The extracted Collins and Sivers moments on ^{3}He are shown together with their statistical errors and systematic error bands for both K^+ and K^- electroproduction. The Sivers moments are compared to theoretical predictions from a phenomenological fit to the world data.

The likelihood was formed by the ϕ_h and ϕ_S dependent yield as shown in Eq. (1),

$$yield(\phi_h, \phi_S) = \rho \cdot \sigma \cdot a_{\pm}(\phi_h, \phi_S)(1 + P \sum_{j=1}^{2} \epsilon_j A_j(\phi_h, \phi_S)),$$
(1)

where ρ is the target density, σ is the unpolarized cross section, $a_{\pm}(\phi_h, \phi_S)$ is the acceptance for target spin state $\pm$, $A_j(\phi_h, \phi_S)$ is the jth azimuthal angular modulation, $\sin(\phi_h + \phi_S)$ or $\sin(\phi_h - \phi_S)$, P is the target polarization, and ϵ_j is the amplitude of each modulation. The ϕ_h and ϕ_S definition follows the Trento Conventions [31]. The MLE method has been used for charged pion analysis [23] and has been checked through Monte Carlo simulations. The results extracted from MLE take into account the unbalanced beam charge associated with two target spin directions and the data acquisition livetime. The ^{3}He Collins and Sivers moments were then obtained by correcting the dilution from unpolarized N$_2$ gas in the target cell. The nitrogen dilution factor is defined as

$$f_{N_2} \equiv \frac{\rho_{N_2} \sigma_{N_2}}{\rho_{^3He} \sigma_{^3He} + \rho_{N_2} \sigma_{N_2}},$$
(2)

where ρ is the density of the gas in the production target cell and σ is the unpolarized SIDIS cross section. The ratio of unpolarized cross sections $\sigma_{N_2}/\sigma_{^3He}$ was measured in dedicated runs on targets filled with known amounts of unpolarized N$_2$ or ^{3}He gas. The f_{N_2} in this experiment was determined to be about 10%.

The dominant systematic uncertainty in our measurement was the contamination from photon-induced charge-symmetric $e^{\pm}$ pairs, of which the e^- was detected in BigBite. The yield of $(e^+, K^{\pm})$ coincidences was measured directly by reversing the magnetic field of BigBite, and hence the contamination of photon-induced electrons in the electron sample was determined. The contamination for K^- detection was 14±7%. Hardly any events were observed in the latter 3 bins for K^+ detection from calibration runs which indicated that the contamination in these bins was small. To be conservative, the contaminations were given by a limit in these bins with the assumption that the contamination decreases linearly through 4 bins. The photon-induced electron contamination for K^+ was determined to be 18.6±8.3%, <10%,

<5%, <3%, respectively for the four x_{bj}-bins. Since this contamination is primarily from photon-induced pair production, it carries the same asymmetry as photon production. The asymmetry contamination correction for K^- and the first bin of K^+ was given by the asymmetry from high energy γ-$K^{\pm}$ coincidence events. Additional experimental systematic uncertainties include: 1) π^- contamination in the electron sample, 2) $\pi^{\pm}$ contamination in the $K^{\pm}$ sample, 3) random coincidence contamination in the $(e^-, K^{\pm})$ coincidence sample, 4) target density fluctuations, 5) detector response drift caused by radiation damage to the BigBite calorimeter, 6) target polarization, and 7) bin-centering effects. The quadrature sum of these uncertainties is quoted as the "experimental" systematic uncertainty for our measurement.

For the asymmetry extraction from Eq. (1), we only included $\sin(\phi_h + \phi_S)$ and $\sin(\phi_h - \phi_S)$ modulations by neglecting other modulations, including $\sin(3\phi_h - \phi_S)$ modulation at twist-2 [32], $\sin(\phi_S)$ and $\sin(2\phi_h - \phi_S)$ modulations at twist-3, Cahn $\cos(\phi_h)$ and Boer-Mulders $\cos(2\phi_h)$ modulations from unpolarized cross section. The leakage from the longitudinal polarized target single spin asymmetry (A_{UL}) due to the small longitudinal component of the target polarization was also neglected. These effects were estimated by varying each term within an allowed range derived from the HERMES proton data [33], assuming that the magnitude of each term for the neutron is similar to that of the proton. These effects were summed in quadrature to yield the "fit" systematic uncertainty, which is dominated by the $\sin(\phi_S)$ term.

The extracted ^{3}He Collins and Sivers moments are shown in Fig. 3 and tabulated in Table II. The error bars represent statistical uncertainties. Experimental systematic uncertainties combined in quadrature from different sources are shown as a band labeled "Exp.". Systematic uncertainties due to neglecting other modulations are shown as a band labeled "Fit". The K^+ Collins and Sivers moments are consistent with zero within er-

ror bars, while for K^- these moments are found to favor negative values at the 2-sigma level.

The Sivers moments from the ^{3}He target are compared to theoretical predictions from a phenomenological fit to the world data [34]. While K^+ Sivers moments are consistent with the prediction, K^- results differ from the prediction at the 2-sigma level. Due to the lack of information on the Collins fragmentation function for kaons, no theoretical predictions on the Collins moments are currently available. Our data on the Collins moments will provide independent inputs for a future global analysis to extract flavor dependent transversity distributions. Although with large uncertainties for the K^- Collins and Sivers moments, the results are still surprising compared to our current knowledge of the effects of sea quarks and unfavored fragmentation functions. Therefore, to fully understand the sea quark flavor dependence of the Collins and Sivers moments, high-precision kaon data are required for transversely polarized proton, deuteron and ^{3}He targets.

In summary, we have reported the first measurement of target single spin asymmetries of charged kaons produced in SIDIS using a transversely polarized ^{3}He target. Our data show that the Collins and Sivers moments for K^+ are consistent with zero within the experimental uncertainties, while the K^- results favor negative values. While the statistics for the 6-GeV E06-010 measurements were limited, experiment E06-010 laid the foundation for future 12-GeV SIDIS experiments at JLab [35]. These future SIDIS experiments will provide us a unique opportunity in mapping the kaon Collins and Sivers moments to much higher precision.

[1] V. Barone et al., Prog. in Part. and Nucl. Phys. 65, 267 (2010).
[2] J. Collins, arXiv:1307.2920 (2013).
[3] J. P. Ralston and D. E. Soper, Nucl. Phys. B 152, 109 (1979).
[4] P. Lenisa, F. Rathmann, et al. (PAX Collaboration), arXiv:hep-ex/0505054 (2005).
[5] A. Bacchetta et al., JHEP 0702:093 (2007).
[6] X. Ji, J.-P. Ma, and F. Yuan, Phys. Rev. D 71, 034005 (2005).
[7] A. Kotzinian, Nucl. Phys. B 441, 234 (1995).
[8] P. Mulders and R. Tangerman, Nucl. Phys. B 461, 197 (1996).
[9] D. Boer and P. J. Mulders, Phys. Rev. D 57, 5780 (1998).
[10] J. Collins, Nucl. Phys. B 396, 161 (1993).
[11] R. Seidl et al. (Belle Collaboration), Phys. Rev. Lett. 96, 232002 (2006).
[12] I. Garzia et al. (BaBar Collaboration), arXiv:1201.4678 (2012).
[13] A. Airapetian et al. (HERMES Collaboration), Phys. Rev. Lett. 103, 152002 (2009).
[14] A. Airapetian et al., Phys. Lett. B 693, 11 (2010).
[15] M. Alekseev et al., Phys. Lett. B 692, 240 (2010).
[16] D. Sivers, Phys. Rev. D 41, 83 (1990).
[17] S. J. Brodsky, D. S. Hwang, and I. Schmidt, Phys. Lett. B 530, 99 (2002).
[18] X. Ji, J.-P. Ma, and F. Yuan, Nucl. Phys. B 652, 383 (2003).
[19] J. C. Collins, Phys. Lett. B 536, 43 (2002).
[20] S. J. Brodsky, D. S. Hwang, and I. Schmidt, Nucl. Phys. B 642, 344 (2002).
[21] M. Alekseev et al., Phys. Lett. B 673, 127 (2009).
[22] X. Qian et al., Phys. Rev. Lett. 107, 072003 (2011).
[23] J. Huang et al., Phys. Rev. Lett. 108, 052001 (2012).
[24] J. Alcorn et al., NIM A 522, 294 (2004).
[25] Y. Qiang, AIP Conference Proceedings 1374, 242 (2011).
[26] F. Bissey, V. Guzey, M. Strikman, and A. Thomas, Phys. Rev. C 65, 064317 (2002).
[27] E. Babcock, I. A. Nelson, S. Kadlecek, and T. G. Walker, Phys. Rev. A 71, 013414 (2005).
[28] X. Qian, Ph.D. thesis, Duke University (2011).
[29] Y. Wang, Ph.D. thesis, UIUC (2011).
[30] J. Huang, Ph.D. thesis, MIT (2011).
[31] A. Bacchetta, U. D'Alesio, M. Diehl, and C. A. Miller, Phys. Rev. D 70, 117504 (2004).
[32] Y. Zhang et al., arXiv:1312.3047 (2013).
[33] M.Diefenthaler, Ph.D. thesis, Desy-thesis-10-032 (2010).
[34] M. Anselmino et al., Eur. Phys. J. A39, 89 (2009).
[35] H. Gao et al., Eur. Phys. J. 126, 1 (2011).

	x_{bj}	Collins moment	Sivers moment
K^+	0.137	0.16±0.13±0.024(0.003)	0.078±0.13±0.017(0.005)
K^+	0.190	0.082±0.083±0.01(0.002)	-0.019±0.083±0.0065(0.004)
K^+	0.250	0.0009±0.063±0.003(0.002)	0.0074±0.063±0.006(0.003)
K^+	0.324	-0.075±0.074±0.006(0.002)	-0.019±0.07±0.006(0.002)
K^-	0.210	-0.21±0.10±0.03(0.009)	-0.25±0.10±0.039(0.01)

TABLE II. Tabulated ^{3}He results for the central kinematical variable x_{bj}. The format for the tabulated results follows "central value" ± "statistical uncertainty" ± "experimental systematic uncertainty (systematic uncertainty due to fit model)".